Heliyon 10 (2024) e29971

Contents lists available at ScienceDirect

Heliyon

journal homepage: www.cell.com/heliyon

Research article

Target location method of intelligent deicing robot based on nonlinear auto disturbance rejection neural network

Lili Kong *, Chunqiu Yi **

College of Modern Science and Technology, China Jiliang University, Hangzhou, 310018, Zhejiang, China

ARTICLE INFO

INDEX TERMS:
Robot
Image processing
Feature extraction
Machine vision
Trajectory

ABSTRACT

A visual navigation scheme for intermittent walking deicing robots was designed to address the issues of multiple iterations, long computation time, and poor real-time performance in the nonlinear optimization of the original SLAM system. A computer image acquisition unit, a computer image processing module, and a visual navigation parameter extraction algorithm were also designed. Implemented a visual navigation system for deicing robots based on image processing. It can meet the navigation requirements of the deicing robot. Simulation and experiments have shown that the method proposed in this paper can quickly and accurately identify abnormal point clouds. The visual servo control scheme constructed in this paper is aimed at robot task operations with unknown system calibration and target depth information. By calibrating the robot vision system, the conversion between camera pixel coordinates and robot base coordinates is achieved, with a transmission frame rate of 53.65 per second; The maximum error in positioning accuracy in space is 10.6 mm. The feature trajectory of visual space is smooth and stable within the camera's field of view, and the end movement of Cartesian space robots is stable without rebound, resulting in high grasping and positioning accuracy.

1. Introduction

Due to factors such as icing and snow accumulation on transmission lines, accidents often occur, such as line dancing and insulator flashover, resulting in significant economic losses and posing a serious threat to the safe operation of the power grid. Traditional manual deicing methods have problems such as high risk and low efficiency. With the development of science and technology, replacing manual deicing with robots has become a trend. However, there are still many urgent problems to be solved at this stage.

In recent years, with the rapid development of robot technology, robots are more and more used in the field of electric power inspection. Using robots to complete the inspection of overhead transmission lines is more efficient than the traditional manual inspection and helicopter inspection, with lower maintenance cost, and at the same time, it can ensure the personal safety of operators [1]. Overhead conductor inspection robot equipped with flaw detection device can carry out nondestructive flaw detection on transmission lines, and ensure the safe and reliable operation of power grid. Location technology is one of the key technologies in the research of overhead conductor inspection robot (hereinafter referred to as inspection robot), and the location accuracy directly affects the precise location of line defects. The project team developed LINES PYX [2], an inspection robot for internal flaw detection of carbon fiber composite conductor. The operation area is about 30 m between the tower and the first spacer, so it is necessary to provide

* Corresponding author.
** Corresponding Author
E-mail addresses: 3204831864@qq.com (L. Kong), yilailai@163.com (C. Yi).

https://doi.org/10.1016/j.heliyon.2024.e29971
Received 30 August 2023; Received in revised form 13 April 2024; Accepted 18 April 2024
Available online 21 April 2024

accurate defect location. At present, the positioning of patrol robot mostly adopts the encoder and other contact relative positioning methods [3], which has the disadvantage of large accumulated error. In order to reduce the cumulative error, researchers use differential GPS for robot positioning [4], which can achieve cm-level positioning accuracy. However, this method has high requirements for the erection of reference stations, and has some disadvantages, such as high cost and difficulty in field deployment.

With the development of machine vision technology, vision positioning methods are widely used in the field of robots. The working environment characteristics of the inspection robot are relatively simple, among which the texture of transmission lines has regular characteristics. In this paper, a visual positioning method of inspection robot based on wire texture is proposed. LK optical flow method [5] is used to track the edge characteristics of wire texture and calculate the running distance of inspection robot on line. In order to improve the positioning performance of the system and track the background features, the tracking results of wire texture are evaluated. The experiment shows that the method proposed in this paper has high positioning accuracy and meets the application requirements. Using agricultural mobile robots for automatic navigation can significantly improve the field operation speed, reduce the production cost, and avoid workers being exposed to harsh environments such as high temperature and high humidity [6]. The agricultural mobile robot based on machine vision navigation has the advantages of high working efficiency, good real-time performance and low system cost, and has become a research focus in the field of agricultural machinery navigation at home and abroad [7]. Navigation datum line extraction is one of the key links of agricultural mobile robot navigation. Real-time and accurate detection of crop row centerline and navigation path can effectively improve the operation speed and accuracy of mobile robot. Mobile robots have more operating space and higher flexibility, and are widely used in various occasions. However, due to the restriction of Brockett's condition [8], mobile robots usually need additional state information to solve the problem of asymptotic stability and feedback stability of the control system caused by their own nonholonomic constraints. The visual servo control technology using visual sensors has the advantages of comprehensive information acquisition and high reliability, which can effectively improve the flexibility and intelligence level of mobile robots in unstructured environments, and provide additional state information to build a feedback control system for mobile robots. Therefore, it has been developed rapidly in recent years [9] Because the indoor environment is generally complex, there are situations such as building block and pedestrian intrusion. Therefore, the indoor positioning technology of mobile robot has gradually attracted attention. Google once combined GPS and Wi-Fi technology [10] to mark the specific location to achieve indoor positioning; Professor Hu of Beijing University of Aeronautics and Astronautics put forward a sensor fusion indoor positioning method based on wireless positioning and monocular vision positioning [11]. Although these methods have obvious effects and good accuracy in indoor positioning, there are many difficulties in practical application due to the problems of high cost of related instruments and equipment, great influence of surrounding environment and cumbersome deployment. In order to solve the shortcomings of accurate positioning of service robots in indoor environment [12] and easy blurring of images when moving at a high speed [13], this paper adopts a positioning method that relies on the integration of IMU (Intertemporal Measurement Unit), inertial measurement unit and monocular vision, namely VIO visual inertial odometry [14]. In this paper, the fusion framework adopts tight coupling, a relatively complex but mainstream research method. Britain's Davision took the lead in proposing the MonoSLAM system which uses the universal motion model to smooth camera motion and pre-estimate the feature points of monocular vision, which greatly improves the application value of robots in real-time 3D positioning and map drawing [15]. Ji et al. [16] put forward ORB-SLAM2 system. Compared with its ORB-SLAM system, the new system optimizes the IMU and monocular vision system at the back end, so that it can make more accurate trajectory planning [17]. In visual SLAM, the SLAM process is described by posture and road signs. The so-called feature points in the image are road signs, and the image features include SIFT [18], SURF [19], ORB, etc. ORB improved the defect that FAST has no directionality, and greatly accelerated the speed of image feature extraction through binary BRIE descriptor, which met the real-time requirement of SLAM. Therefore, this paper adopts ORB feature points and feature extraction and matching methods. This paper mainly innovates the algorithm of the back-end optimization part of the current visual SLAM, applies the improved Dog-Leg algorithm on the basis of the original nonlinear optimization algorithm, and designs a method to calculate the radius of the trust area based on the damping factor update. Finally, it is applied to the YOBY robot and tested in the actual scene.

Tele-operated engineering robot refers to the engineering machinery that the operator manipulates the remote manipulator to follow the movement of the main manipulator in different places to complete the task in complex and dangerous environment [20], which can be applied to aviation, rescue, disaster, nuclear environment and other fields [21]. In order to improve the quality of teleoperation, telepresence prompt technology based on hearing, vision and force perception is necessary. Scholars at home and abroad have carried out many researches on visual cue technology of teleoperation engineering robot [22]. In Ref. [23], a man-machine interface based on augmented reality technology is added to the teleoperation construction robot system. The system uses virtual images instead of video images, which provides operators with multiple perspectives, so that operators can complete tasks more simply and safely. In reference [24], a robotic arm with six cameras is used in the teleoperation engineering robot for immediate explosive discharge, and a complete three-dimensional scene is reconstructed in real time by using multi-view information. Although the above research enhances the operator's sense of presence, the multi-view visual feedback system is complex and costly. In Ref. [25], a stereo vision processing method based on image superimposition is proposed by using a three-eye camera to collect images of hydraulic engineering robots. By superimposing three images acquired in real time, the visual cue effect is achieved, the operator's sense of presence is enhanced, and the operation efficiency is improved. However, due to the large amount of data transmitted by pictures, the time delay is large. In Ref. [26], a binocular stereo vision prompting method of teleoperated hydraulic engineering robot is proposed, which uses the points on the sticker as feature points for matching, but the actual effect will be affected by the sticker effect and illumination, and the robustness is not strong enough. Aiming at the problems of complex structure, time delay and low technical robustness of the existing visual cue system of teleoperation hydraulic engineering robot, this paper proposes a visual cue technology of teleoperation hydraulic engineering robot based on attitude identification [27]. The image of teleoperation hydraulic engineering robot is obtained by camera, and the displacement of hydraulic cylinder of teleoperation hydraulic engineering robot is obtained by

key point recognition stacked hourglass network model and attitude recognition neural network (AR-NN) model, which drives virtual engineering robot to realize visual cue to operators. The experiment proves its effectiveness.

However, existing research mostly focuses on robots working in specific environments, and there is relatively little research on the uneven quality distribution of parts to be sorted in actual production, edge burrs, and overlapping and shadows caused by random placement of workpieces. Based on this, the author of this article builds an unordered sorting platform and proposes a machine vision based collaborative robot task target positioning system to achieve pose recognition and sorting of unordered workpieces.

2. Construction of material method data set

2.1. Visual slam system

The visual SLAM system in this paper is mainly composed of five functional modules: sensor data processing and acquisition, front-end visual odometer optimization, back-end optimization, loop detection and map building, as shown in Fig. 1.

The specific system flow of this paper is shown in Fig. 2. The sensors commonly used in the first module are cameras (monocular camera, binocular camera, TOF depth camera) IMU (Inertial Measurement Unit), laser radar [28] and so on. In the second module, the visual odometer roughly estimates the motion of the camera according to the similarity of several adjacent image information, and through the corresponding algorithm processing, provides the initial value for the back end. In the back-end optimization of the third module, because the front-end visual odometer can only estimate the local camera pose through adjacent images, the incremental map constructed by this method has accumulated errors, which requires the back-end optimization to construct a globally consistent map to improve the accuracy of the map and pose estimation. Among the optimization methods, the extended Kalman filter algorithm estimates the state of the current moment by the state of the previous moment, while the nonlinear optimization algorithm optimizes the data of all moments together, so the nonlinear optimization algorithm greatly improves the estimation accuracy.

The function of the module, loop detection, is to judge whether the robot has been to the same position, thus forming a closed loop, adding constraints, reducing the calculation amount and accumulated error of the back-end optimization, and correcting the posture of the robot. Finally, map construction. SLAM system [29] can construct 2D grid map, 2D topology map, 3D point cloud map and 3D grid map according to the different application scenarios and actual needs.

The specific system flow of the point cloud and polishing trajectory is shown in Fig. 2.

(1) data preprocessing: the camera is a 30Hz monocular camera, which adopts ORB method to extract and match features, and uses binary descriptors to mark features; The IMU data is integrated to obtain the position, velocity and rotation of the current moment, and the pre-integration increment, Jacobian matrix and covariance term are calculated at the same time.
(2) Initialization: firstly, estimate the pose of all frames and the position of landmark points in the sliding window by using the motion recovery structure (SFM), then fuse with IMU data to recover the real scale information, and finally solve the initialization parameters (such as gravity, velocity, gyro bias);
(3) Back-end nonlinear optimization: putting visual constraints, IMU constraints and marginal prior information constraints into a large objective function for nonlinear optimization, and solving PVQ and bias;
(4) Loop detection: using DBoW2 to detect one frame every three key frames, which is equivalent to skipping two frames to perform loop detection once, and repositioning after successful detection;
(5) Global pose map optimization: only the pose of the camera in the sliding window is obtained by the optimization in the sliding window, and the loop detection can only correct the pose of the camera in the sliding window by using the loop frame, that is, only the local pose is optimized, but the pose of the whole camera is not corrected. Considering the global consistency of map trajectory, the camera pose map optimization should be optimized globally in addition to local optimization.

The front end of SLAM is also called visual odometer (VO). According to whether or not features need to be extracted, the realization methods of VO can be divided into feature point method and direct method. For the optical flow method, the premise is that the time is continuous, and the motion is small and the gray scale is constant, so it can't be tracked well when the camera moves or rotates on a large scale. The feature point method used in this paper is considered as the mainstream method of visual odometer. When the motion is too large, as long as the matching point is still in the image, it will not cause frame loss, and it is more robust than the optical flow method.

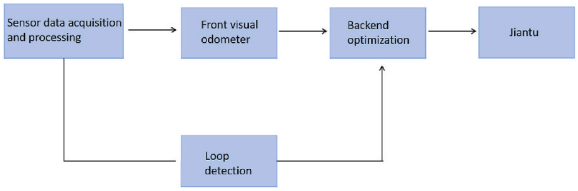

Fig. 1. SLAM overall process.

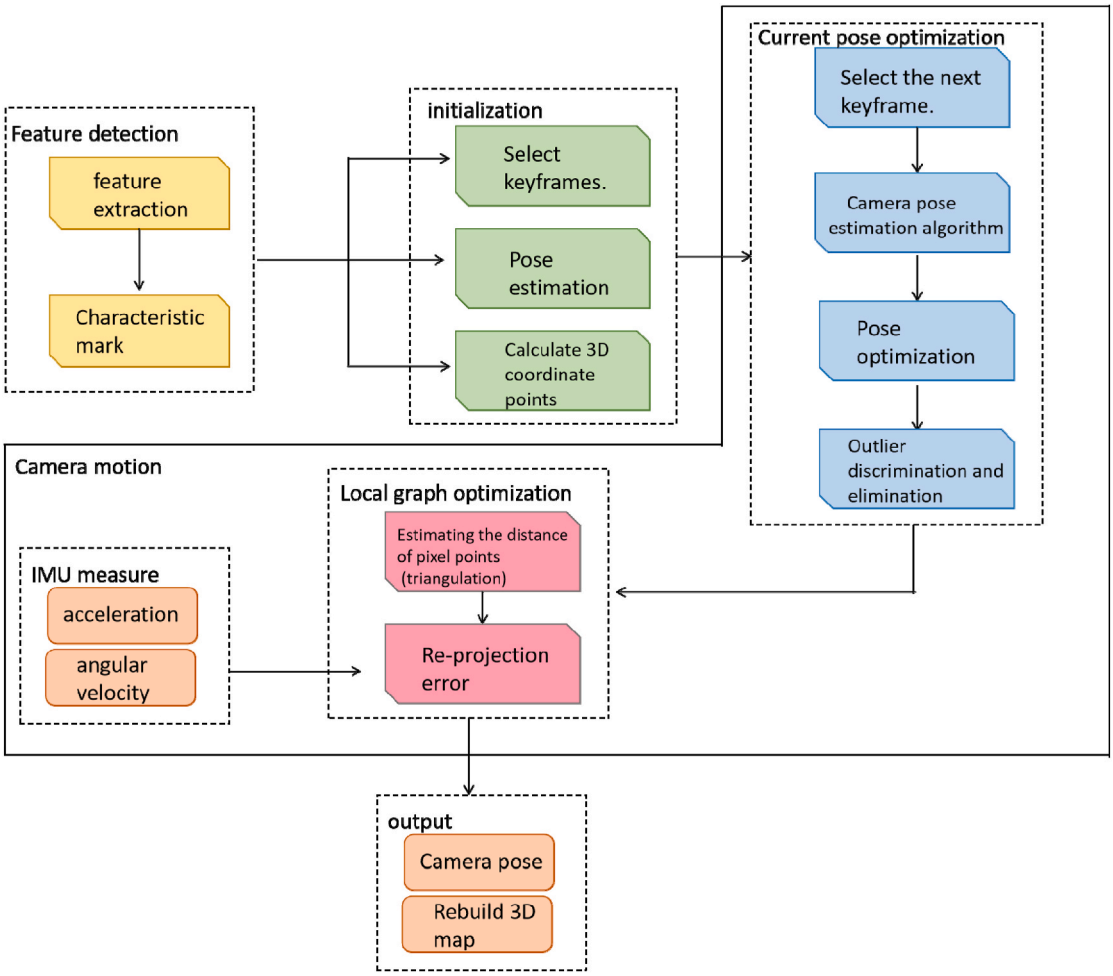

Fig. 2. System flow of this paper.

2.2. *Design of robot visual navigation process for deicing*

The working environment of the deicing robot studied is a fruit orchard. In order to realize the visual navigation of the robot, it is necessary to analyze and study the surrounding environment of the orchard to plan the design process of visual navigation. The visual navigation process of deicing robot is shown in Fig. 3.

The visual navigation process of deicing robot includes orchard environment analysis, characteristic target determination, deicing robot walking mode determination, hardware platform construction, image acquisition and processing, navigation information acquisition, deicing robot motion control and visual navigation software design, etc. This chapter mainly studies the first four parts.

1) Analysis of orchard environment. Orchard environment is the working environment of deicing robot, which plays an absolute role in the mobile platform of deicing robot. Therefore, it is necessary to analyze and study the orchard environment first. Orchard environment is different from other environments and can be divided into roads, fruit trees and fences, as shown in Fig. 4.

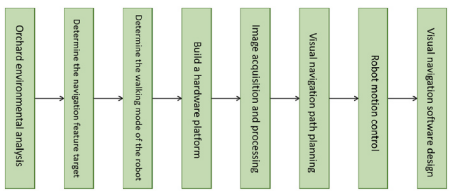

Fig. 3. The visual navigation flow chart of agricultural robot.

2) Determine the navigation feature target. In order to facilitate the picking operation of deicing robot, it is generally necessary to treat the orchard road.

It can be seen from Fig. 4 that in addition to the road area, there are areas such as fruit tree rows and ridges, fruit trees and fences in the orchard environment. Among them, there are obvious differences in characteristics between road areas and other areas. Therefore, this study takes the feature difference between orchard road and fruit tree ridge image as the feature target.

3) Determine the walking mode of deicing robot. De-icing robots usually need a long distance from fruit trees, and some fruit trees are tall, and the fruits to be picked are widely distributed. Picking robots need to walk intermittently, that is, picking a piece of fruit and moving forward for a certain area. Therefore, the moving interval distance of the deicing robot is set to 2 m, as shown in Fig. 5.

1) selection of DSP processor. In order to realize the visual navigation system of deicing robot, TMS320C5545(DSP) is selected as the core processor of the system. The processor is a high-speed, high-performance and low-power processor, which can realize the control and application of portable audio and video, industrial control, wireless transmission, fingerprint identification and medical devices. TMS320C5545 mainly includes CPU, FFT hardware accelerator [30], DMA, power control unit, RAM and ROM. It has the characteristics of high reliability and can meet the industrial control and low power consumption requirements of deicing robot vision navigation system.

2) Camera and lens selection. The camera is an important device for the visual navigation of deicing robot. The CCD camera with low noise figure ratio, fast photographing speed and moderate cost is selected. When the deicing robot moves in the orchard environment, the whole machine will vibrate because of uneven road or vibration of mechanical hand-held picking.
3) Visual navigation scheme design. Relying on computer, artificial intelligence, machine vision, obstacle sensor and Beidou positioning system, the deicing robot can pick the target fruit without human operation. Because the orchard environment is complex, in order to accurately realize the visual navigation system of deicing robot, it is necessary to monitor the surrounding environment with visual sensors in many directions. The robot vision navigation control scheme for deicing is shown in Fig. 6.

The deicing robot realizes the visual navigation of the picking path through CCD industrial camera, DSP and its own model, and uses the intelligent control system to realize the motion control function. Robot deicing vision navigation adopts multi-core DSP processor, and its image processing framework is shown in Fig. 7.

When the deicing robot processes the image, it will store the video image in the external memory of the system, then distribute the image data to different DSP cores for image depth processing, and finally save the processed data information to the external memory [31].

2.3. Visual cue technology

The overall architecture of the visual positioning method of overhead transmission line inspection robot proposed in this paper is shown in Fig. 8, which is mainly divided into three parts: conductor identification, feature extraction and feature tracking. The wire recognition part detects the position of the transmission wire in the image, and extracts this part of the image as the region of interest (ROI) for subsequent feature extraction. The feature extraction part preprocesses and adaptively detects the edge of the traverse image to obtain the texture features of the traverse. At the same time, feature points are extracted from the background image for subsequent tracking calculation. In the feature tracking part, the texture features and background features are tracked by optical flow respectively, and the tracking result of wire texture is evaluated according to the proportional relationship of optical flow vectors, and the position of feature points is updated for subsequent calculation. Finally, according to the mapping relationship between pixel points and object movement, the displacement of the robot relative to the wire is obtained.

The visual cue system of teleoperation hydraulic engineering robot studied by the author is shown in Fig. 9.

Transmit to image processing PC. Image processing PC uses KPR-SHN model and AR-NN model to recognize the image, obtain the displacement information of the hydraulic cylinder, and transmit it to the operation terminal through the communication network. At

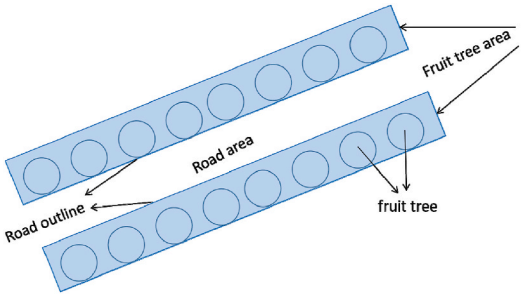

Fig. 4. The schematic diagram of orchard environment.

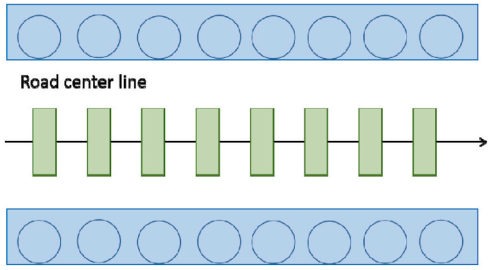

Fig. 5. The walking mode diagram of agricultural robot.

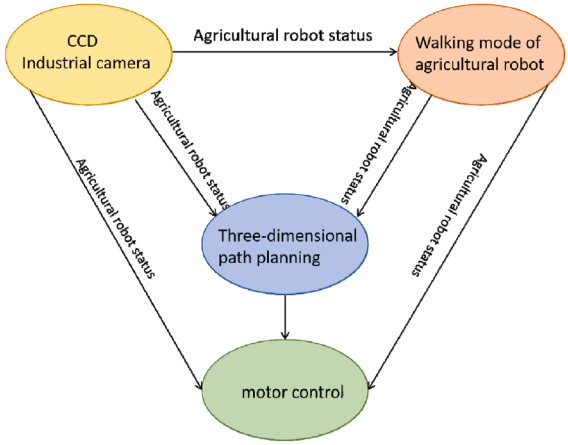

Fig. 6. The vision navigation control scheme of agricultural robot.

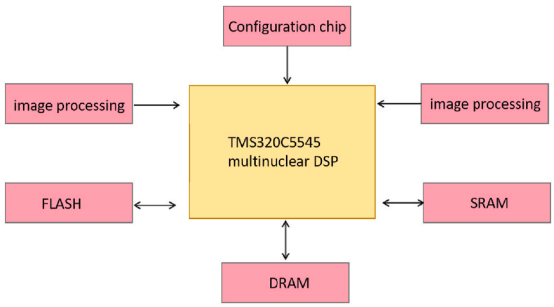

Fig. 7. The image processing frame of agricultural robot.

the operation end, the control robot PC drives the virtual robot to move according to the displacement information of the hydraulic cylinder, and provides visual cues to the operator. The operator uses the force feedback handle.

Remote operation of engineering robot by controlling robot PC. This system can not only make the operator have a sense of presence, but also reduce the operation error caused by the video image transmission delay. The visual cue process is shown in Fig. 10.

Before the operation, it is necessary to obtain the image data, the corresponding key point coordinate data and the displacement data of the hydraulic cylinder of the teleoperation hydraulic engineering robot, and train the stacked hourglass networks KPR-SHN and AR-NN. When working, the image information of the hydraulic engineering robot acquired in real time is input into the trained KPR-SHN model [32] to identify key points, and the key point information is input into the trained AR-NN model to identify the displacement of the hydraulic cylinder, which drives the virtual engineering robot to provide visual cues.

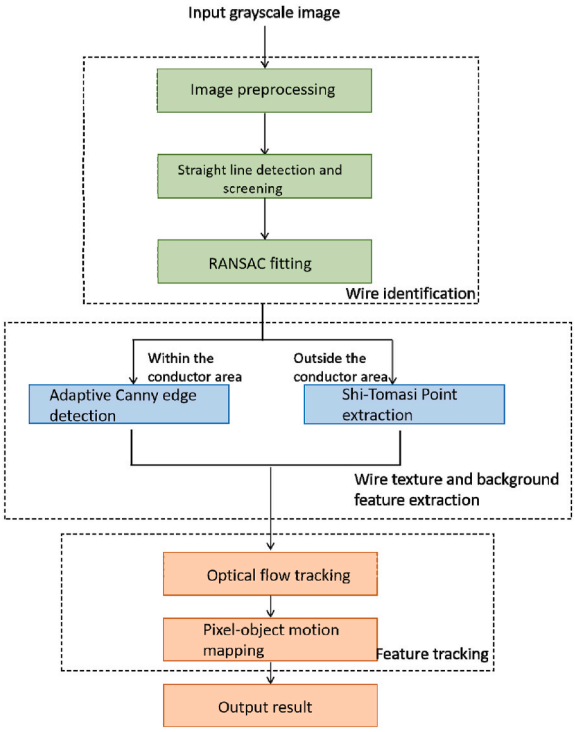

Fig. 8. Overall architecture of vision positioning system.

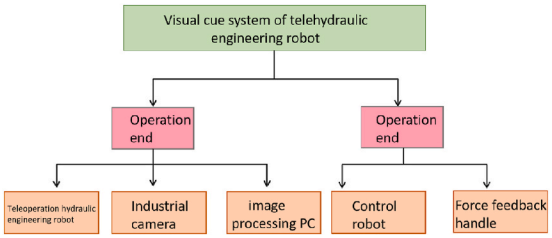

Fig. 9. Visual cue system.

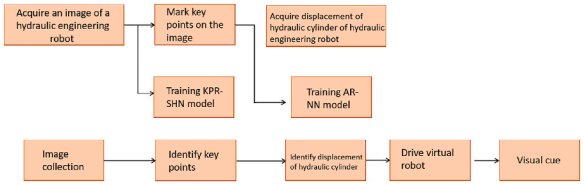

Fig. 10. Visual cue process.

3. The research method of this paper

3.1. Design of computer image acquisition unit

The image acquisition unit of robot deicing vision navigation system is composed of DSP controller based on computer control, CCD industrial camera, lens, light source and sensor, and image acquisition mainly depends on CCD industrial camera. In this study, the industrial camera MV-SUA501GC-T of Maidewei is selected, which adopts full-frame scanning line by line, integrates signal processing and basic recognition algorithm, and can preprocess the image first. Visual navigation system diagram Image acquisition block diagram is shown in Fig. 11.

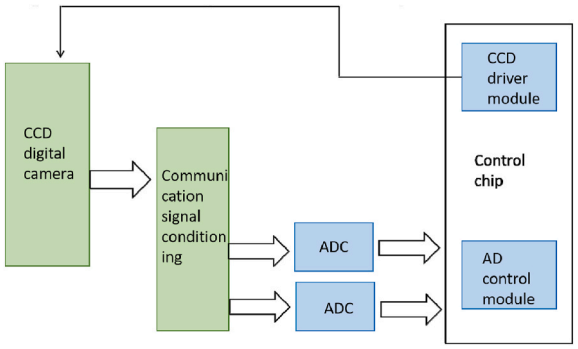

Fig. 11. The image acquisition block diagram of visual navigation system.

The computer image processing module is based on the computer segmentation according to the chromaticity, and the background area can be segmented according to the chromaticity segmentation, thus realizing the distinction between the road area and the ridge of fruit trees. Chromaticity segmentation is divided into the following processes.

1) normalize brightness and chromaticity, and normalize them to [0, 25] in the range.
2) carry out image segmentation processing. When the absolute value A of adjacent pixels is less than the threshold D of chromaticity division, they are classified into the same block area, otherwise, they are classified into the next classification. The regular expression of image segmentation is shown as formula (1):

$$\begin{aligned} \mathrm{d}_i &= \left\{ d_{i,top}, a\left(c_i, c_{i,top}\right) < D \right. \\ \mathrm{d}_i &= \left\{ d_{i,left}, a\left(c_i, c_{i,left}\right) < D \right. \\ \mathrm{d}_i &= \left\{ d_{level}, a\left(c_i, c_{i,top}\right) > D, a\left(c_i, c_{i,left}\right) > D \right. \end{aligned} \tag{1}$$

among, d_i and d_{level} They are the segmentation value and average value of the ith pixel respectively.; c_i Is the pixel value of the grayscale image. $c_{i,top}$、 $c_{i,left}$ The values at the top and left of the pixel, respectively.

3) Divided chromaticity region classification. The same chromaticity will be normalized to the same area, and the average depth value of chromaticity division is shown as formula (2):

$$a_k = \frac{1}{n_k} \sum_{i \leq k} m_i \tag{2}$$

Among, a_k is the average depth of the kth chromaticity division. m_i Is chromaticity value.

The architecture of the image processing module of the vision system depends on the structure of the computer image algorithm, and the overall framework is shown in Fig. 12. Chroma segmentation consists of image sharpening, segmentation and filtering. Chroma sharpening mainly sharpens the image. Chroma segmentation is carried out according to the rules of image segmentation. Depth filtering ensures that the image optimization is carried out in the same chroma segmentation area.

The depth image filtering framework of the vision system is shown in Fig. 13. Depth image filtering is to compare and analyze the filtered chroma segmentation results in memory with the values after the comparator, then further segment the results to get the average value, correct the depth image, and finally save the results.

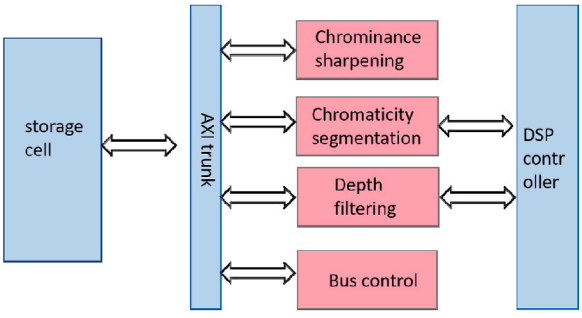

Fig. 12. The image processing module framework of vision navigation system.

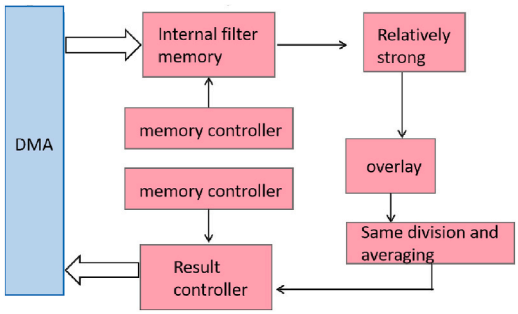

Fig. 13. The filter frame of depth image of visual navigation system.

3.2. Accurate positioning

Firstly, the image of the indoor experimental ceiling was collected by a monocular wide-angle camera, and four monocular cameras were used to image the indoor surrounding environment.

Information collection. Then, the texture features of the image are extracted, the center point of the current image and the current position of the robot are found and recorded to form an information base. Collect environmental information at different positions in the laboratory for coarse matching and positioning in the later stage.

(1) Generation of fingerprint information base

Grayscale the collected indoor environment image (size: 640 × 480); The image is divided into 8 × 8 average sub-blocks by block method, each sub-block is processed by DCT transformation [33] and inverse transformation [34], and the coefficient of 4 × 4 in the upper left corner is kept, and the correlation coefficient is used to combine into a new matrix. At this time, the image size is reduced to 320 × 240; The four reduced environmental images are spliced into a new matrix D of 1280 × 240 in a fixed order, and the feature vector P in the image is extracted by whitening and singular value decomposition [35], so as to achieve the purpose of reducing redundancy and dimensionality. Finally, let G = PD, and a global feature vector G of 1280 × 1 is obtained (please refer to Ref. [36] for specific formula derivation); Obviously, four images of each location can be represented by a global feature description vector as fingerprint information, and the fingerprint information of images of multiple locations forms a fingerprint information base.

(2) ceiling information processing

In indoor scenes, because the structure of the ceiling is simple, there is no intrusion of objects and it is not easily disturbed, but its characteristic information is less, so it is necessary to process the image information. The edge detection algorithm is used to extract the edge of the ceiling image, and then the improved adaptive median filter is used to optimize the image, so as to extract the texture information of the ceiling in the test picture. Finally, the center point of the image is recorded and marked.

By processing the ceiling image in the test image, the texture features and the coordinates of the center point of the image are obtained and marked. Then, the Gaussian function with $\sigma = 1.5$ is used to smooth the gradient to reduce the influence of noise. Harris key point detection algorithm is used to extract the key points in the test image and the matching result image, ANMS [37] method is used to select the best key points, and the matching result is optimized by improved GMS. So as to achieve the best matching result. Taking the best matching result as the relationship model between the two images, the ceiling information in the original data set obtained by matching is fused and spliced with the ceiling information in the test image through perspective transformation [38], thus obtaining a fused image containing two image information. Because perspective transformation [39] is based on the principle that three points of perspective center, image point and target point are collinear, the linear relationship in the original image can still be maintained in the transformed image after perspective transformation (please refer to Ref. [40] for perspective transformation principle). Then, the fused image is processed to find the corresponding points of the original two images in the fused image, and the positions of the center points of the original two images in the fused image are calculated, and the distance between the two points is obtained by formula (3), which is its displacement.

$$|\text{distance}| = \left(\sqrt{x_1} - x_2\right)^2 + \left(\sqrt{y_1} - y_2\right)^2 \tag{3}$$

Finally, the coordinate values of the four corners of the superimposed test chart image are calculated through the transformation matrix, and any adjacent two corners are calculated. Δx,Δy,Calculate the deflection angle by formula (4):

$$angle = \arctan\frac{|\Delta y|}{|\Delta x|} \tag{4}$$

The displacement difference is calculated by detecting the position difference of the center of the original two images in the fused image, and the perspective transformation matrix of the fused two images is sent to the computer.

People's current deflection angle, so as to achieve accurate positioning, the overall process as shown in Fig. 14.

3.3. Virtual engineering robot

The displacement data of hydraulic cylinder output by AR-NN model is transferred to the virtual engineering robot operation simulation platform to reconstruct the 3D scene. The reconstruction process is shown in Fig. 15. The modeling process of virtual engineering robot involves SolidWorks, 3DMAX and OpenGL, etc. The specific steps are as follows: firstly, the components of teleoperation hydraulic engineering robot are created in SolidWorks, then converted into 3ds format in 3DMAX, finally imported into OpenGL, and the hydraulic cylinder of teleoperation hydraulic engineering robot is modeled by OpenGL.

Due to the complex environment of power lines, the robotic arm monitoring camera is prone to local reflections near the power cables during image capture. Such reflections can damage the image quality of power cable images and blur the edges. In addition, if the surveillance camera is directly exposed to sunlight, it can cause the entire foreground of the image to darken. These impacts are controlled by no legal entity, and in order to improve the reliability of robot monitoring cameras in some complex environments, it is necessary to optimize visual algorithms. Homomorphic filtering is widely used for image correction under uneven illumination. Homomorphic filtering not only reduces low frequencies, but also increases high frequencies, reduces lighting changes, and makes detailed edges clearer. Applying homomorphic filtering methods to preprocess power cable images to reduce uneven light interference on the images.

Visual navigation parameters are important parameters of deicing robot walking. Based on the feature value extraction of image by image acquisition and processing module, this paper realizes the parameter extraction of visual navigation system according to computer image algorithm. The image of fruit tree rows and ridges obtained by CCD camera is shown in Fig. 16.

To establish the rectangular coordinate system of the image, L intersects with the X and Y axes to form included angles θ and α, respectively. Assume that the intersection coordinates of L and X of fruit tree row ridge are (x, y), and the distance between this point and O is d. After the positional relationship between θ and L, the calculation expression of navigation parameters is shown as formula (5):

$$\begin{cases} d = |x| \\ \alpha = 90 - \theta\theta > 90 \\ \alpha = \theta - 90\theta \leq 90 \end{cases} \tag{5}$$

Calculate that navigation parameters of the deice robot d and α,According to the change of parameters and thresholds, the next action of deicing robot can be planned. Robot deicing can be divided into straight-ahead and turning.

Drive straight. When the parameters satisfy formula (6) and formula (7), say. The navigation line and angle of the deicing robot are within the threshold range, so Nong Robots should continue to walk in the current direction.

$$|d| < d_t \tag{6}$$

$$\begin{cases} (d < -d_t) \cap (\alpha > 0) \\ (d > d_t) \cap (\alpha < 0) \end{cases} \tag{7}$$

Turn left and right. When the parameter satisfies formula (8), it means that the navigation line and angle of the deicing robot have some deviation, so the deicing robot should start to adjust its steering.

$$\begin{cases} (d < -d_t) \cap (-\alpha_t < \alpha < 0) \\ (d > d_t) \cap (0 < \alpha < \alpha_t) \end{cases} \tag{8}$$

After extracting the visual navigation parameters of the deicing robot, the deicing robot can be actually controlled according to its driving state.

4. Experiment and analysis

4.1. Visual navigation effect of deicing robot

In order to test the actual navigation effect of the deicing robot visual navigation system, the system was tested experimentally. The experiment was conducted in an apple planting garden, and the distance between two rows of ridges was 3 m. During the test, in order to record the actual movement position of the deicing robot; Particularly, the actual midline position of the deicing robot chassis is

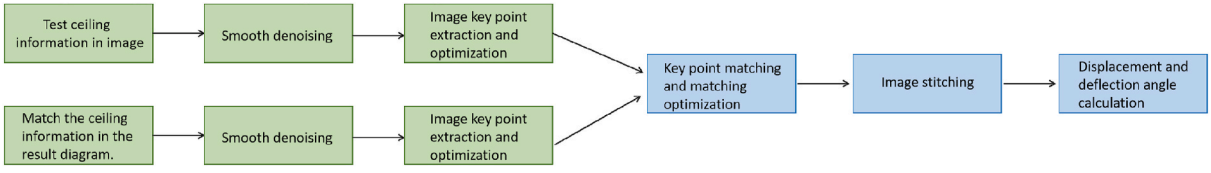

Fig. 14. Accurate positioning process.

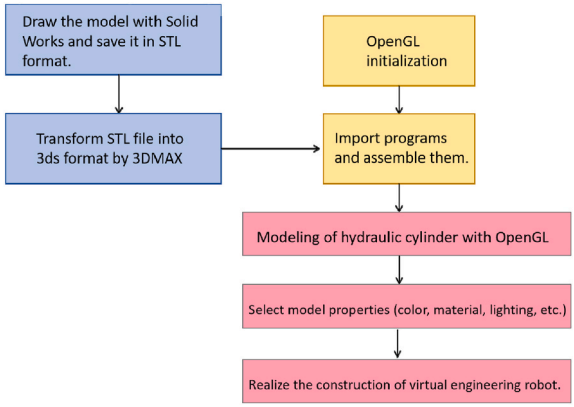

Fig. 15. Construction process of virtual engineering robot.

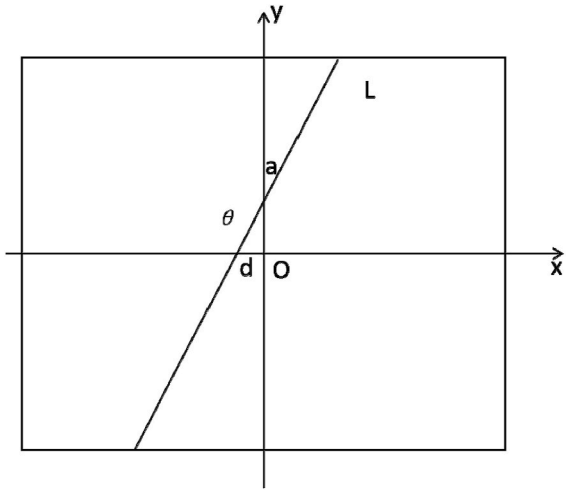

Fig. 16. The ridge image of fruit trees obtained by CCD camera.

drawn by chalk. Every time the robot walks 2 m, the actual navigation position of the deicing robot is recorded by labeling paper, and then the distance between the midline position and the left row ridge is measured with a tape measure. In order to compare whether the moving speed of the deicing robot will affect the navigation results, experiments were conducted at 0.3 m/s and 0.5 m/s respectively, and the results are shown in Table 1.

It can be seen from Table 1 that when the deicing robot moves forward at a speed of 0.3 m/s, the average distance between the robot centerline and the left row ridge is 147.4 cm, with a deviation of 4.4 cm; When the current row speed is 0.5 m/s, the average distance

Table 1
The table of the experimental results of the influence of the moving speed of agricultural robot on the navigation.

experiment sequence	speed of advance 0.3 m/s		speed of advance 0.5 m/s	
	actual distance	error	actual distance	error
1	153	3	145	−5
2	148	−2	144	−6
3	147	−3	141	−9
4	144	−6	138	−12
5	141	−9	144	−6
6	140	−10	151	1
7	145	−5	153	3
8	150	0	156	6
9	152	2	150	0
10	154	4	148	−2
average value	147.4	4.4	147	5

between the robot centerline and the left row ridge is 147 cm, with a deviation of 5 cm. The experimental results show that the navigation error will increase when the moving speed of the deicing robot increases, and the average lateral deviation of the robot is within 10 cm, which can meet the navigation requirements of the deicing robot.

4.2. Experimental melt

In order to verify the proposed visual cue method, the project members established a visual cue experimental platform. The hardware system of the experimental platform is mainly composed of a hydraulic engineering robot, an image processing PC, a control robot PC, an industrial camera and a force feedback handle, etc., in which the industrial camera is parallel to the plane where the mechanical arm of the engineering robot rotates at 0.

The attitude of the attitude identification model is measured at any five moments during the actual grasping operation, and the expansion and contraction of three hydraulic cylinders and the rotation angle of one hydraulic cylinder of the hydraulic engineering robot are taken as experimental data. The results are shown in Table 2 and Table 3. In the experiment, the detection speed of the displacement of the actual hydraulic cylinder reaches 9 frames/s. Compared with the measured results, the error of attitude identification is within 8 %.

On average, it takes 0. 11 s for the visual cue platform to process a frame of image and finally make the same action by the virtual robot. The average detection time of KPR-SHN model is 0. 031 s, that of AR-NN model is 0. 023 s, and that of driving the virtual robot is 0. 055 s. Therefore, the visual cue system can solve the problem of time delay, and the accuracy can meet the requirements.

4.3. Dynamic performance test of navigation algorithm

In order to evaluate the dynamic performance of the navigation path recognition algorithm, the tractor navigation platform was used to track the path at the speed of 0. 8 m/s, 1. 2 m/s and 1. 6 m/s, respectively. In the experimental corn field, the average plant height is about 30 cm, the row spacing is 60 cm, and the track length is 25 m. The high-precision global positioning system (GPS) is installed at the top center of the tractor to collect the system's motion track, and the camera is installed on the front counterweight frame of the tractor. Both the GPS and the camera are located on the tractor's central axis, and the output frequency of GPS positioning data is 926. The rate of jiangsu journal of agricultural sciences, Vol. 36, No.4, 2020 is 2 Hz. Before the test, GPS is used to start from the starting point of the navigation path, and one point is collected at a certain distance until the end point, so that the reference information of the tracking path can be obtained. In order to ensure the validity of navigation data, the three speed tracking tests were repeated five times, and the one with the largest lateral deviation under each speed condition was selected for analysis.

It can be seen from Table 4 that under different weed densities, the difference between the parameters (intercept and slope) of the navigation path extracted by artificial bee colony algorithm and the reference navigation path is the smallest; In Table 5, the error between the navigation path extracted by Hough transform algorithm and the reference navigation path is the largest, followed by the least square method, which shows that the anti-interference ability of artificial bee colony algorithm to weeds is stronger than the other two algorithms.

The experimental results show that the navigation line recognition method based on artificial bee colony algorithm proposed in this study can quickly and accurately identify the navigation datum line, which has good real-time and accuracy compared with Hough transform algorithm, is insensitive to weed noise compared with least square method, and has strong anti-interference ability.

It can be seen from Fig. 17(a)(b)(c) that under the same speed condition, the lateral deviation of the three navigation line extraction algorithms fluctuates up and down based on 0, among which the Hough transform algorithm has the largest fluctuation range, followed by the least square method and the artificial bee colony algorithm has the smallest fluctuation range.

As can be seen from Table 6, under the three navigation speeds, the maximum lateral deviation and average lateral deviation of Hough transform algorithm and least square method are higher than those of artificial bee colony algorithm. The main reason is that weed noise interference reduces the navigation path accuracy fitted by these two algorithms, resulting in increased tracking error. The experimental results show that in the dynamic environment, the navigation datum line extracted by artificial bee colony algorithm proposed in this study can make agricultural navigation robot track the navigation path quickly and accurately, and has good dynamic characteristics.

5. Conclusion

In this paper, the visual navigation system of deicing robot is studied, the navigation characteristic target and walking mode of robot are analyzed, and the computer image acquisition and processing unit is designed, and the extraction method of visual navigation parameters of deicing robot is studied. The results show that when the moving speed of deicing robot increases, the navigation error will increase, and the average lateral deviation of the robot is within 10 cm, which can meet the navigation requirements of deicing robot. Aiming at the problems of complex system structure, network transmission delay and low robustness in the application of video sensing in teleoperation hydraulic engineering robot, the system is upgraded by introducing industrial camera and deep learning algorithm. The intelligent identification of abnormal areas and areas to be polished is realized. Based on this method, the coordinate data of areas to be polished can be obtained, and the automatic planning of robot polishing trajectory is completed by using offline simulation software. At the same time, some special areas are optimized manually, and the offline programming of intelligent polishing system is completed. This method can automatically identify and extract abnormal areas of typical sheet metal parts, and through system integration, the offline programming of areas to be polished is realized, which realizes automation and intelligence of

Table 2
Experimental data of swinging boom.

serial number	Swing angle value		Telescopic amount of boom hydraulic cylinder/mm	
	predict	reality	predict	reality
1	5.67	5.31	748.68	713.63
2	−4.56	−4.26	791.36	739.15
3	8.66	7.94	823.53	768.47
4	15.35	14.14	736.58	703.97
5	7.56	7.03	742.84	717.45

Table 3
Experimental data of bucket and gripper.

serial number	Telescopic amount of bucket hydraulic cylinder		Telescopic amount of hydraulic cylinder	
	predict	reality	predict	reality
1	630.63	596.75	49.08	45.68
2	589.68	561.46	91.36	86.65
3	613.39	578.85	43.53	41.75
4	713.37	686.63	108.52	101.34
5	658.39	610.78	58.56	55.25

Table 4
Comparison of guidance line parameters of different algorithms.

testing environment	Hough Transformation algorithm		method of least squares		Artificial bee colony algorithm		Reference navigation path	
	slope	Intercept (pixels)	slope	Intercept (pixels)	slope	Intercept (pixels)	slope	Intercept (pixels)
Low weed density	8.0	−4832	−102.2	71 351	−32.8	23 591	−21.9	15 815
High weed density	7.8	−5022	37.6	−24 056	−38.3	25 108	−41.8	27 809

Table 5
Error of navigation path by different algorithms.

testing environment	Error (pixel)		
	Hough Transformation algorithm	method of least squares	Artificial bee colony algorithm
Low weed density	11 967	957	204
High weed density	15 945	1372	578

polishing process and reduces manual intervention.

Declarations

Conflicts of interest

The authors declare no conflict of interest.

Data availability statement

Data presented in this work can be made available on request from the corresponding author.

CRediT authorship contribution statement

Lili Kong: Validation, Resources, Methodology, Data curation. **Chunqiu Yi:** Writing – original draft, Software, Project administration.

Declaration of competing interest

The authors declare the following financial interests/personal relationships which may be considered as potential competing interests:

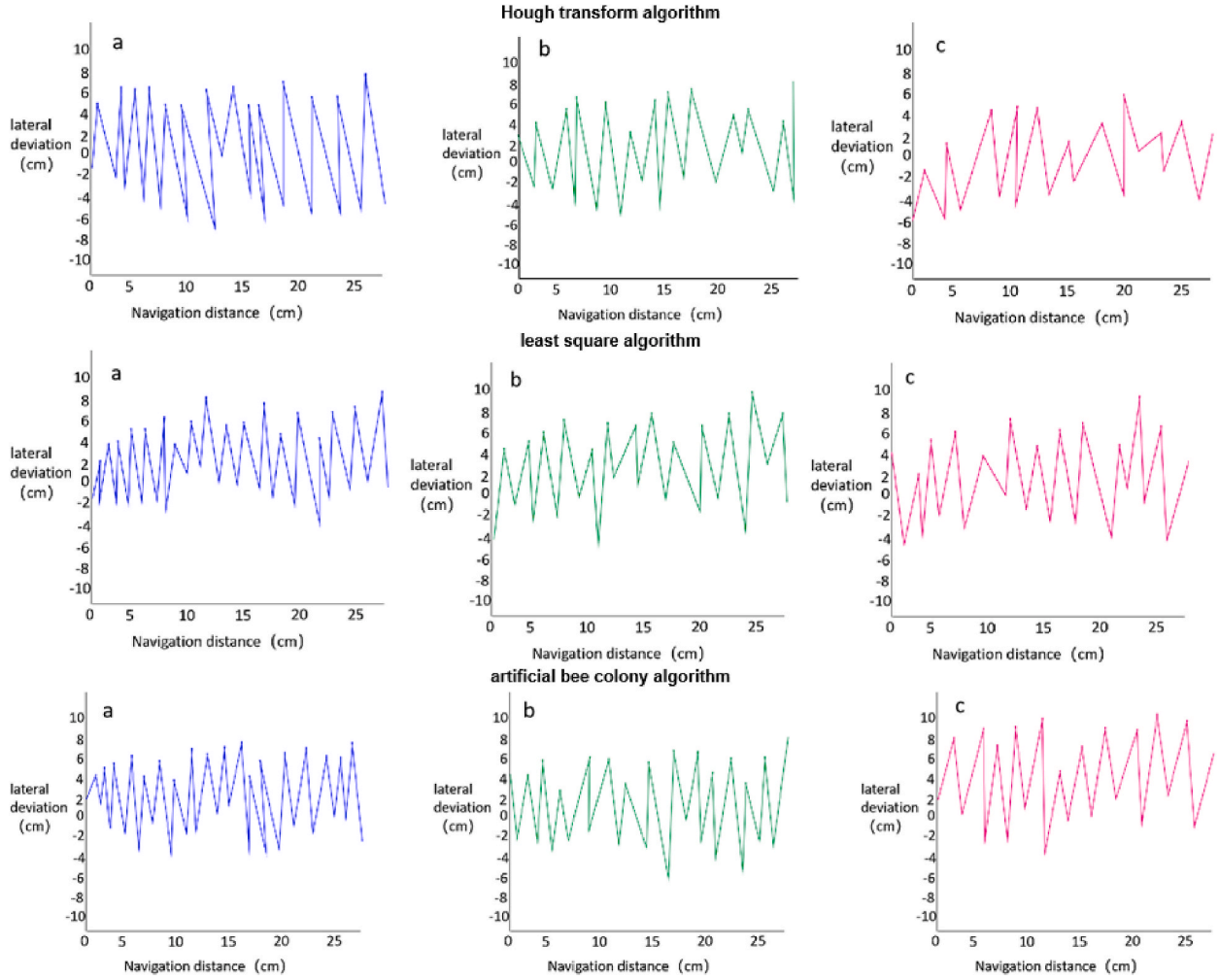

Fig. 17. Tracking results of guidance line by comparison of Three Algorithms.

Table 6
Errors of navigation path tracking by three guidance line recognition algorithms under different speeds of agricultural mobile robot.

Mobile agricultural machinery Driving speed of people (m/s)	Hough Transformation algorithm		method of least squares		Artificial bee colony algorithm	
	Maximum lateral deviation (cm)	Average lateral deviation (cm)	Maximum lateral deviation (cm)	Average lateral deviation (cm)	Maximum lateral deviation (cm)	Average lateral deviation (cm)
0.8	7.2	3.1	5.7	2.5	4.6	1.9
1.2	11.4	5.2	8.1	3.1	6.8	2.4
1.6	14.6	6.2	10.6	4.7	8.9	4.0

Hongxu Xian reports was provided by Inner Mongolia University of Technology.

References

[1] Xiaofang Wu, Ran Duan, Liwei Yang, Hongjie Duan, Analysis of evaluation index of sci-tech journals based on Keras neural network model, Tianjin Science and Technology 49 (8) (2022) 102–106.
[2] Cai Chaozhi, Chi Yaolei, Guo Lubin, Zhonghang Zhang, Jinxin Bai, Research on frame structure fault diagnosis based on CEEMDAN and neural network, Modern Electronic Technology 45 (16) (2022) 80–86.
[3] Lili Wu, Xiaoqing Gu, Yuqing Xing, Aiying Lin, Jianbin Pan, Yan Fengming, Application of Convolutional Neural Network in the recognition of insect stinging potential waveform, Modern Electronic Technology 45 (16) (2022) 181–186.
[4] Hongjie Sun, Zhenhua Zhao, Linxian Huang, Liting Xing, Jie Hao, Zhenjiang Luo, Application of multivariate LSTM neural network model in groundwater level prediction, People's Yellow River 44 (8) (2022) 69–75.
[5] Changxin Cao, Research on the Target Positioning of Yarn Hanging System Based on Machine Vision [D], wuhan textile University, 2022.

[6] Sinan Lu, Jiacai Huang, Fangzheng Gao, Li Yibo, Tian Chen, Target positioning method of integrating Beidou satellite positioning system with VSLAM, J. Nanjing Inst. Technol. 20 (2) (2022) 24–30.
[7] Jingxu Zhao, Chen Zhao, Zhou Feng, Cooperative target location method based on master-slave autonomous underwater vehicle mobile networking, Journal of Electronics and Information 44 (6) (2022) 1919–1926.
[8] Li Hanxing, Design of MEMS Acoustic Sensor Array Target Positioning System [D], Xi 'an University of Technology, 2022.
[9] Yazhou Zhang, Li Xiaoqing, Xiaobo Huang, Evaluation model of enterprise innovation ability based on RBF-BP compound neural network, Journal of Xiamen University of Technology 29 (6) (2021) 51–56, https://doi.org/10.19697/j.cnki.1673-1673404076.
[10] Zewu Peng, Cai Xiong, Qiuyong Yang, Huaquan Su, Research on optimized compression algorithm of deep convolution neural network based on FPGA, Computational Technology and Automation 40 (4) (2021) 74–78.
[11] H.U. Sheng-bin, A method of highlighting target location in remote sensing images based on big data, Jingwei Tiandi (6) (2021) 46–49.
[12] Yue Peng, Zuqiang Meng, Lina Yang, A speech enhancement method based on GRU neural network, J. Guangxi Univ. (Nat. Sci. Ed.) 46 (6) (2021) 1533–1548.
[13] Liu Zuo-shi, Mu Hong-shu, Yang Guo-wei, Research on robot positioning technology based on target recognition, Sensors and Microsystems 40 (12) (2021) 31–34+39.
[14] Shuai Zhang, Songwei Han, Guanbing Bai, Zhongyu Liu, Analysis and research on positioning accuracy of UAV photoelectric platform based on reference point guidance, Electronic Technology and Software Engineering (24) (2021) 214–219.
[15] Li Yang, Research and Implementation of Indoor Positioning Technology Based on RFID [D], Nanjing University of Posts and Telecommunications, 2021.
[16] Yanxing Ji, Xianjun Ding, Research on improvement of adaptive phase difference estimation algorithm for underwater target location, Ship Electronics Engineering 41 (11) (2021) 158–163.
[17] Dongliang Wang, Research on Insulator Defect Detection Method Based on Convolutional Neural Network [D], Xi 'an Shiyou University, 2021.
[18] Rong Xinrui, Research on Fiber-Optic Multi-Target Positioning and Identification System Based on Mach-Zehnder Interference [D], Chongqing University, 2021.
[19] Licheng Qu, Jiao Lu, Yihua Qu, Haifei Wang, Intelligent allocation and location algorithm of moving target based on fuzzy neural network, Computer Science 48 (8) (2021) 246–252.
[20] Huiling Zhu, Image Target Recognition and Location of Substation Safety Monitoring Based on Convolutional Neural Network [D], South China University of Technology, 2021, https://doi.org/10.27151/D.CNKI.
[21] Zejin Lu, Research on Two-Stage Target Location Method Based on Convolutional Neural Network [D], Hunan University, 2021.
[22] Tang Tang Tang, Research on Event-Based Target Positioning and Recognition Model [D], Sichuan University, 2021, https://doi.org/10.27342/D.CNKI.GSCdu.20000.000000000005.
[23] Qin Xiao, Chengcheng Huang, Yu Shi, Zhaoqi Liao, Xinyan Liang, Chang 'an Yuan, Research progress of image classification based on convolutional neural network, Guangxi Sci. 27 (6) (2020) 587–599+696.
[24] Mang Zhou, Li Guohua, Chenguang Li, Chenlong Jiang, Guo Qixiang, Research on the prediction of enterprises' resumption of production based on BP neural network, Jilin Electric Power 48 (6) (2020) 22–25.
[25] Seimi Zhang, Hui Lin, Xiangren Long, Wetlands classification method using full convolution neural network and Stacking algorithm, Journal of Agricultural Engineering 36 (24) (2020) 257–264.
[26] Wei Huang, Research on Optimization Algorithm of Node and Target Location in Wireless Sensor Network Based on RSSI [D], Nanjing University of Posts and Telecommunications, 2020.
[27] Wei Gao, Zhongyi Yin, Shuling Huang, Wenjiao Zhang, Zixuan Jin, Analysis of the positioning error of the geographic target of the ultra-small UAV [C]. Proceedings of the 2020 Academic Annual Meeting of the Science and Technology Committee of China Academy of Aerospace Electronics Technology, 2020, pp. 50–53, https://doi.org/10.26914/C.CNKIHY.2020.
[28] Zhenwu Kuang, Research on the Positioning and Tracking Technology of Moving Target Based on UWB [D], Guilin University of Technology, 2020.
[29] Chunlei Lu, Path Planning of McNamun Wheel Robot in Unknown Environment and its Target Detection and Positioning [D], Dalian Maritime University, 2020, https://doi.org/10.26989/D.CNKI.GDLHU.20000.000000000005.
[30] Bing Zhao, Research on Location and Classification Technology of Ground Objects Based on Airborne Multi-Source Remote Sensing Data [D]. University of Chinese Academy of Sciences (Xi 'an Institute of Optics and Fine Mechanics, Chinese Academy of Sciences), 2020.
[31] Jianfeng Wen, Qin Yihai, Research on visual target location based on convolutional neural network, Modern Information Technology 4 (22) (2020) 113–115.
[32] Jinwei Liu, Research on the Method of Identifying and Locating Sea Targets by Unmanned Aerial Vehicle Formation [D], Harbin Institute of Technology, 2020.
[33] Cheng Zhuo, Weak Supervision Target Location Based on Convolutional Neural Network and its Application [D], Chongqing University of Posts and Telecommunications, 2020.
[34] Haipeng Zhao, Research on the Technology of Target Identification, Detection and Location Based on Portable Sensors [D], Information Engineering University of Strategic Support Force, 2020.
[35] Yu Yichun, Face recognition based on neural network algorithm, Electronic Technology and Software Engineering (24) (2019) 247–248.
[36] Hui Yuan, Research on Image Retrieval Based on Feature Performance Enhancement and Target Location [D], Xi 'an University of Technology, 2019.
[37] Ganlu, Design and Implementation of Visual Positioning System Based on Convolutional Neural Network [D], University of Chinese Academy of Sciences (Shenyang Institute of Computing Technology, Chinese Academy of Sciences), 2019.
[38] Le Zhang, Research on the Algorithm of Abnormal Target Detection and Location in Deep Neural Network Video [D], Yanshan University, 2019, https://doi.org/10.27440/D.
[39] Ling Wang, Research on Multi-Target Location Based on Convolutional Neural Network [D], Chang 'an University, 2019.
[40] Junjie Jia, Research on Target Attribute Recognition Method Based on Convolutional Neural Network [D], shenyang ligong university, 2019.